

ASSESSMENT OF DESIGN BASIS EARTHQUAKE GROUND MOTIONS FOR NEAR-FAULT CONDITIONS

Mustafa ERDIK¹ And Eser DURUKAL²

SUMMARY

Near-fault ground motions are strongly influenced by the earthquake faulting mechanism exhibiting distinct long period pulses with amplitudes depending on the orientation of the site with respect to the rupture direction. The paper describes a hybrid procedure developed for the assessment of the design-basis ground motion for important engineering structures near major faults. The procedure relies on the combination of the deterministically obtained low frequency (DC-1Hz) ground motion with the stochastically simulated high frequency components. A descriptive example is provided to illustrate the application of this procedure.

INTRODUCTION

Near-fault ground motions are strongly influenced by effects due to the seismic source (e.g. radiation pattern, directivity, rupture model, stress drop) and effects due to wave propagation (e.g. stratigraphy, geo-morphology, lateral scatterers, fault zone as waveguide). At periods longer than about 1s, near-fault (in the vicinity of about 10km, few wavelengths) ground motions are strongly influenced by the earthquake faulting mechanism and orientation of the site. At these periods the ground motions may follow certain radiation patterns, predicted by equivalent double-couple source models, and exhibit distinct long period pulses with amplitudes depending on the orientation of the site with respect to the rupture direction. For cases where the rupture front propagates toward the site and the direction of fault slip is aligned with the site., the so-called "forward rupture directivity effect" is manifested by a long period large amplitude horizontal ground motion pulse normal to the strike of the fault. In the near-fault region of an earthquake the ground motions have distinct pulse-like characters (fling). Empirical evidences of this phenomenon can be observed in the strong motion data from several earthquakes including 1992 Erzincan, 1994 Northridge and 1995 Kobe events [Somerville, 1996]. Widely use predictive earthquake engineering tools, such as empirical attenuation relationships and spectral shapes fail in the assessment of such near fault motions. Although special stipulations have been advocated for the code-based earthquake resistant design of near-fault-sited building structures, no routinely applied procedures exist for the assessment of design basis earthquake ground motions for important facilities to be built near, or crossing, faults.

GROUND MOTION SIMULATION PROCEDURE

Deterministic theoretical predictions of the ground motion can be achieved by convolution of the Green's Functions and the slip function. Green's functions can be calculated through empirical and synthetic means. Although certain predictions can be made for the total slip and the mode of faulting, associated with the DBE (Design Basis Earthquake Ground Motion), no prediction can be made regarding the rupture characteristics. This necessitates the consideration different rupture models. Such deterministic predictions cannot be extended into

the frequency regions above 1Hz, since, high frequency ground motions are controlled by the heterogeneities in the fault rupture, which cannot be a-priori accounted for in a deterministic manner. This requires either the use of

¹ Bogazici University, Kandilli Observatory and Earthquake Research Institute, Turkey. E-mail: erdik@boun.edu.tr

² Bogazici University, Kandilli Observatory and Earthquake Research Institute, Turkey. E-mail: durukal@boun.edu.tr

stochastic source models or the stochastic treatment of the high frequency components in the ground motions. Based on these considerations a hybrid procedure is developed for the assessment of the time history of the design basis earthquake ground motion, compatible with the stipulated source parameters, for important engineering structures near major faults. The procedure addresses the low and high frequency components of the ground motion separately and then combines the two motions in an intelligent way. The basic tenets of the simulation procedure are chosen to: (1) Preserve the deterministic displacement shape; (2) Satisfy the corresponding theoretical Fourier Amplitude Spectrum and; (3) Yield a coda shape in conformance with applicable empirical findings. Furthermore, the peak ground acceleration (PGA) and the pseudo spectral relative velocity (PSRV) values should be favorably compared against those obtained from empirical attenuation relationships for conformity. The essential elements of the procedure can be listed as follows:

1. Assessment of the source parameters of the DBE motion associated with the corresponding return period for specific conditions of site and seismicity.
2. Deterministic assessment of the low frequency (DC-1Hz) ground motion, at the outcrop of a reference soil layer, due to rupture of seismic faults.
3. Use of a Boore (1983)-type stochastic simulation method to complement the deterministic low frequency ground motion with high frequency (1Hz-50Hz) components.
4. Combination of the two parts of ground motion to yield a site specific simulation for a frequency range of DC-50 Hz.
5. Site response analysis, if required, to include the local wave propagation effects in the soil media above the reference soil layer.

APPLICATION CASE STUDY

This case study involves the assessment of the seismic hazard and the design basis ground motion associated with the envisaged container port in Izmit Gulf (Figures 1 and 2). The proximity of the site to a major fault system makes a thorough assessment of the earthquake potential imperative to the safety of the container port. For simulation of the ground motion a multi-phased approach described above is used. On the basis of the earthquake hazard analysis the following scenario earthquakes and the associated PGA values have been obtained.

Table 1 Deterministic Earthquake Scenarios and PGA (g) values.

SCENARIO EVENT	Boore et al. (1994) (Random)		Campbell and Bozorghnia (1993)	
	50-Percentile	84-Percentile	50-Percentile	84-Percentile
Design Basis ($M_S = 7.2, 8\text{km}$)	0.37	0.62	0.48	0.63
($M_S = 6.8, 2\text{km}$)	0.41	0.65	0.68	0.86

SIMULATION OF GROUND MOTION

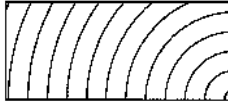
A state-of-the-art approach utilized for the earthquake resistant design of important civil engineering structures located near active faults is the deterministic simulation of the design basis ground motion compatible with the stipulated source parameters. The simulation process yields reliable ground motion within the frequency band generally between 0 and 1Hz. For complementing the simulated motion with higher frequency components a stochastic procedure based on rational spectral and time domain bounds are used. The ground motion is simulated for the competent soil layer.

Low Frequency Ground Motion (DC-1Hz)

The discrete wave number approach in conjunction with a propagator-based formalism is used for the synthesis of seismic ground motion [Deodatis, Shinozuka and Papageorgiou, 1990], [Theoharis and Deodatis, 1994]. The methodology is based on the work of Lamb (1904), Bouchon (1979), Chouet (1987) and Dunkin (1965). The discrete wave number technique is used to propagate waves due to the rupture of an extended seismic source through a 3-D layered half-space. The method is deterministic in the description of the wave propagation. It can be probabilistic or deterministic in the description of the rupture of the seismic source. With this method it is possible to calculate the near-field and far-field 3-D seismic ground motion at any point of a layered viscoelastic half-space, such that the spatial variability of ground motion at distances comparable to the dimensions of

engineering structures can be estimated. All types of waves (body and surface) are accounted for in the formulation of the problem. The ground motion time histories with frequencies up to 3 Hz can be calculated. The estimation of the extent and magnitude of permanent ground deformation is also possible, which is very important in the earthquake response of large-scale engineering structures with relatively low natural frequencies of vibration, such as bridges. The wave radiation from the source is decoupled into P-SV and SH motions and then treated separately in 3-D wave plane propagation using the propagator-based approach of Chouet (1987). Analytical expressions calculated for the displacements due to unidirectional unit impulses are used to compute the solutions for double couples associated with a strike-slip and dip-slip fault. These solutions are finally combined and integrated over the fault area to yield the seismic ground motion. The problem requires two basic input information groups; the ground description and the source description. The ground is described in terms of layers. The formulation necessitates depth, S-wave velocity, P-wave velocity, density and the attenuation factor Q of each layer characterizing the earth structure in the study area. The seismic source is described in terms of its dimensions and location within the earth structure and in terms of its rupture details. The source can either be in one of the layers or in the half-space. The source is discretized into a number of point sources on which the slip is modeled by a double couple. Each double couple can have a different final slip (strike-slip, dip-slip, or both), a different rise time and a different rupture initiation time. The evolution of slip at a certain location on the fault plane as a function of time is described by the dislocation function. Haskell's model uses a ramp function for the dislocation defined by the rise time and the final slip. For the scenario earthquake considered, two segments on the North Anatolian Fault are determined to be critical for the project site. The first segment ("fs59", Figure 2), called the Sapanca segment in this study, is assumed to experience a 40 km long by 15 km deep rupture. The second segment ("fs62", Figure 1,2), called the Yalova segment, is assumed to rupture along a 70 km long by 15 km deep plane. On the basis of the Wells and Coppersmith (1994) study these fault plane dimensions correspond to a $M = 6.8$ earthquake for the Sapanca segment and to a $M = 7.2$ earthquake for the Yalova segment. An earth model including the Moho discontinuity is considered. The classic Haskell type ramp function is considered as the dislocation function. The source is described by 32x12 point sources in both segments. The size of point sources is 1250 m x 1250 m in the Sapanca segment and 2187 m x 1250 m in the Yalova segment. There is a 1.5m final strike-slip and 0.05 m final dip-slip in the Sapanca segment. In the Yalova segment there is only a strike-slip of 2.5 m and no dip-slip. The rise times are assumed as 1.0 second for all point sources on the Sapanca segment and 1.2 seconds for all point sources on the Yalova segment. The fault plane is vertical ($\delta=90^\circ$) in both cases. The numerical values given above correspond to an $M = 7$ earthquake on the Sapanca segment and to an $M = 7.5$ earthquake on the Yalova segment. The rupture propagation pattern in all cases is circular. Two cases of rupture patterns are assumed to take place on the Sapanca segment and one case on the Yalova segment. The cases, as summarized in Table 2, differ in the location of the hypocenter. The rupture velocity is 2800 m/s.

Table 2 Description of the rupture pattern cases.

	SLIP TYPE	RUPTURE PATTERN
Sapanca Segment – 1	Strike-slip + Dip-slip	
Sapanca Segment – 2	Strike-slip + Dip-slip	
Yalova Segment	Strike-slip	

As for the computational parameters 512x512 wave numbers are used in the wave number domain with an upper cut-off wave number of 0.002073 rad/m for the Sapanca segment and 0.001745 rad/m for the Yalova segment. 128 frequencies are used in the frequency domain with an upper cut-off frequency of 0.95 Hz for the Sapanca segment and 0.8 Hz for the Yalova segment. The locations where the displacements are simulated, correspond to three equispaced points along the long axis of the container port, almost perpendicular to the modeled fault segments, as indicated in Figure 2. These points are approximately 650 m apart from each other. The displacement traces in three directions are obtained at three locations on the project site for three cases. Maximum displacement values for the three cases at three locations are summarized in Table 2. The velocity and acceleration values in Table 2 are obtained by differentiation of the displacement traces and should be treated

with care due to the low resolution and due to the narrow frequency band defined in obtaining the displacement records. Results illustrate that large permanent displacements as a result of the scenario earthquakes are to be expected at the project site. Final fault parallel displacements are 1.2 m, 0.85 m and 0.5 m at respective points 1,2 and 3 in Case 1 (Sapanca segment, bilateral rupture); 1.2 m, 0.85 m and 0.4 m at the same points in Case 2 (Sapanca segment, unilateral rupture) and 0.15 m for all points in Case 3 (Yalova segment, bilateral rupture). The fault perpendicular final permanent displacements are in the order 0.05 m and is practically the same for Cases 1 and 2 at all points. In Case 3 the permanent fault perpendicular displacements are about 0.10 m at all points. In the up-down direction the permanent displacements are about 0.02 m and are practically the same at all three points for Cases 1 and 2. For Case 3 permanent vertical displacement is about 0.01m at all points. These results show that in the fault parallel direction relative displacements in the order of 80 cm are to be expected along the long axis of the project. Although there are some permanent displacements to be expected in the fault perpendicular and up-down directions these values are not critical to the project in terms of their relative values. Results indicate that the maximum displacements are in the order of 1.2 m, maximum velocities in the order of 1 m/s and maximum accelerations in the order of 0.3 g. It should be noted that these values, especially the peak ground acceleration, inherently reflect the frequency bandwidth (0-1 Hz) of the simulation process. With higher frequency resolutions the acceleration values will reach higher values. Fault parallel displacements at Point 1 of Case 1 provide maximum ground motion and deserve consideration. The simulations obtained at Point 1 in the fault parallel direction of Case 1 are thus chosen as the “design basis” record. The fault parallel, fault perpendicular and up-down components associated with this “design basis” simulation will be coded as (P1X1, P1Y1 and P1Z1) and are shown in Figures 3 and 4.

High Frequency Ground Motion (1Hz to 50Hz) and Combination with the (DC-1Hz) Motion

Earthquake ground motion deterministically generated using the discrete wave number approach provides a frequency resolution under 1Hz. For complementing this motion with frequency components above 1Hz a stochastic simulation procedure is utilized. The basic tenets of the simulation procedure are chosen: (1) to preserve the deterministic displacement shape; (2) to satisfy the corresponding theoretical Fourier Amplitude Spectrum; and (3) to yield a coda shape in conformance with applicable empirical findings. Furthermore, the peak ground acceleration (PGA) and the pseudo spectral relative velocity (PSRV) values are checked against those obtained from empirical attenuation relationships for conformity. The methodology used is akin to [Boore, 1983] and [Silva and Green, 1989]. The stochastic simulation procedure uses the theoretical Fourier Amplitude spectrum and the coda shapes. The theoretical Fourier Amplitude Spectrum shape of the acceleration of the shear wave field can be computed in terms of: Shear Wave Propagation Velocity, Mass Density and Quality Factor (for Anelastic Attenuation) in the Half Space, Hypocentral Distance, Seismic Moment (as a function of Moment Magnitude), Low Frequency Corner Frequency (as a function of Shear Wave Propagation Velocity and Stress Drop) and High Frequency Corner Frequency. The Fourier Amplitude Spectrum (FAS) has been modeled following [Brune, 1970], A stress drop of 100 bars is considered. In order to account for the decrease of the spectral shape above a high frequency corner frequency, due to near field attenuation and/or source process, a low-pass fourth order Butterworth filter is used. A near-surface amplification [Boore, 1986] due to seismic impedance differences is also considered. The quality factor, $Q(f)$, which controls the anelastic attenuation in the half-space is assumed to be frequency independent and assigned a value of 300. The methodology utilized for the stochastic simulation of high frequency components can be described by the following steps:

- 1) Generate the theoretical FAS of ground displacement for given conditions;
- 2) Generate the empirical coda shape for given conditions;
- 3) Generate a Gaussian white noise with zero mean;
- 4) Multiply (2) and (3);
- 5) Adjust the amplitude of (4) such that its FAS yields unit amplitude on the average (this can be met if its variance is equal to its bandwidth and (2) has a unit squared area);
- 6) Add the deterministic displacement shape (DC to 1Hz) to (5) and re-adjust the amplitude;
- 7) Obtain the Fourier Amplitude Spectrum (FAS) of (6);
- 8) Obtain the Fourier Phase Spectrum (FPS) of (6);
- 9) Multiply (1) and (6) to obtain the FAS of the simulated motion;
- 10) Compute the inverse Fourier transform (simulated time series) using FPS; from (6) and FAS from (9); and
- 11) Generate another Gaussian white noise and repeat steps (3) to (10).

The ensemble of FAS obtained from (10) and (11) will, at the limit, resemble the FAS at step (1).

RESULTS

Acceleration, velocity and displacement time histories, simulated on the basis of the ground displacement obtained from the P1X1 and P1Y1 models, are provided in Figures 5 and 6. The similarity of the velocity and the displacement traces to those provided in Figures 3 and 4 for the P1X1 model can be seen. The peak of the acceleration record is 0.52g, which agrees with the deterministic PGA obtained (Table 1). The pseudo relative velocity (PSRV) response spectrum of the simulated acceleration time history is plotted in tri-partite format in Figure 7 for 0, 2, 5, 10 and 20% damping ratios. The empirical PSRV response spectra computed with Boore et al., (1993) spectral attenuation relationship, using the DBE scenario of $M = 6.8$ earthquake at 2 km fault distance, soil class B and 5% damping, is provided in Figure 8. The conformity between the two response spectra for 5% damping in the medium and high frequency regions can be observed. These comparisons do prove that the simulation criteria set forth in the first paragraph of this section is adhered by this methodology.

CONCLUSION

The several variants of the simulation procedure have been tested. The application of the simulation procedure is illustrated with a comparative example on the assessment of the DBE ground motion for a major container port facility near the North Anatolian Fault. It has been shown that the hybrid procedures yields ground motions with sufficiently reliable low frequency components. It should also be noted that the low frequency limit of the pseudo relative velocity approaches asymptotically to the maximum (may be DC component) ground displacement.

REFERENCES

- Barka, A.A. and K. Kadinsky-Cade (1988), Strike-slip Fault Geometry in Turkey and its Influence on Earthquake Activity, *Tectonics*, 7-3, 663-684.
- Boore, D.M. (1983), Stochastic Simulation of High-Frequency Ground Motions Based on Seismological Models of the Radiated Spectra, *Bull. Seism. Soc. Am.*, V.73, pp.1865-1894.
- Boore, D.M. (1986), The Effect of Finite Bandwidth on Seismic Scaling Relationships, in *Earthquake Source Mechanics*, S.Das, J.Boatright and C.Scholz, eds., Geophysical Monograph 37, AGU, Washington, D.C., pp.275-283.
- Boore, D.M., W.B. Joyner and T.E. Fumal (1994), Estimation of Response Spectra and Peak Accelerations from Western North American Earthquakes: an Interim Report Part 2. USGS Open-File Report 94-127.
- Bouchon, M. (1979), Discrete Wave Number Representation of Elastic Wave Fields in 3 D Space, *Journal of Geophysical Reserach*, V. 84, No. B7, pp. 3609-3614.
- Brune, J.N. (1970), Tectonic Stress and the Spectra of Seismic Shear Waves from Earthquakes, *J. Geophys. Res.*, v.75, pp.4997-5009.
- Campbell K.W. and Y. Bozorgnia (1993), Near-source attenuation of Peak horizontal acceleration from worldwide accelerograms recorded from 1957 to 1993. *Proc., Fifth US Nat. Conf. Earthq. Eng.*, Chicago.
- Chouet, B. (1987), Representation of an Extended Seismic Source in a Propagator Based Formalism, *Bulletin of the Seismological Society of America*, V. 77, No. 1, pp. 14-27.
- Cluff, L.S., K.J. Coppersmith and P.L. Kneupfer (1982), Assessing Degrees of Fault Activity for Seismic Microzonation, *Proc. 3rd Int. Earthq. Microzonation Conf.*, Seattle, Wash., II, 113-118.
- Deodatis, G., M. Shinozuka and A.S. Papageorgiou (1990), Stochastic Wave Representation of Seismic Ground Motion: I- FK Spectra, *Journal of Engineering Mechanics*, ASCE, V. 116, No. 11, pp. 2363-2379.

Dunkin, J.W. (1965), Computation of Modal Solutions in Layered, Elastic Media at High Frequencies, Bulletin of the Seismological Society of America, V. 55, No.2, pp. 335-358.

Lamb, H. (1904), On the Propagation Tremors at the Surface of an Elastic Solid, Philosophical Transactions of the Royal Society of London, V. A203, pp. 1-42.

Saragoni, G.R. and G.C. Hart (1974), Simulation of Artificial Earthquakes, Earthq. Eng. and Struct. Dyn., v.2, pp.249-267.

Silva W.J. and R.K.Green (1989), Magnitude and Distance Scaling of Response Spectral Shapes for Rock Sites with Applications to North American Tectonic Environment, Earthquake Spectra, v.5, pp.591-624.

arođlu, F., A. Boray and Ö. Emre (1987), Active Faults of Turkey, Mineral Res. & Explor. Inst., Turkey, Unpublished Report 8643, 349 pp.

Somerville, P. G.; Smith, N. F.; Abrahamson, N. A. (1996) Accounting for near-fault rupture directivity effects in the development of design ground motions, Eleventh World Conference on Earthquake Engineering [Proceedings], Pergamon, Elsevier Science Ltd.

Theoharis, A. and G. Deodatis (1994), Seismic Ground Motion in a Layered Half-Space due to a Haskell-type source. I: Theory, Soil Dynamics and Earthquake Engineering, V. 13, No. 4, pp. 281-292.

Wells, D.L. and K.J. Coppersmith (1994), New Empirical Relationships among Magnitude, Rupture Length, Rupture Width, Rupture Area, and Surface Displacement, Bull. Seism. Soc. Am., v.84, pp. 974-1002.

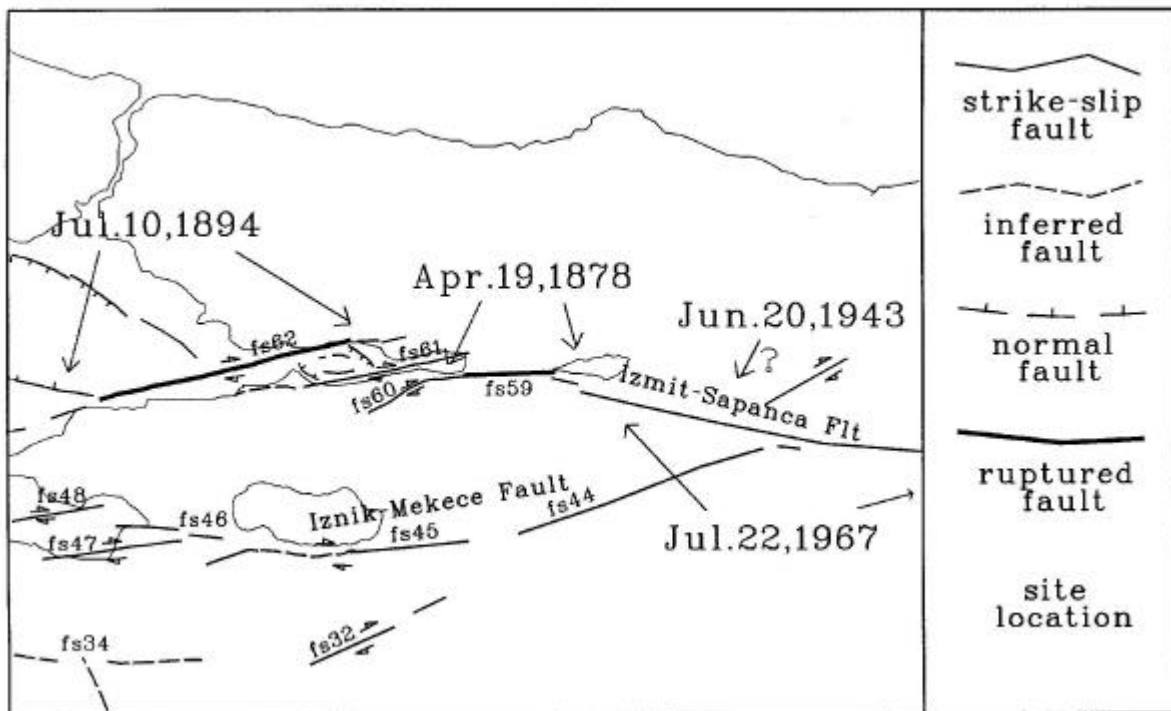


Figure 1 Tectonic map of İzmit region, major faults, including tectonic lineaments numbered 'fs59', 'fs61' and 'fs62' and recent major earthquakes, adapted from Barka and Kadinsky-Cade (1988)

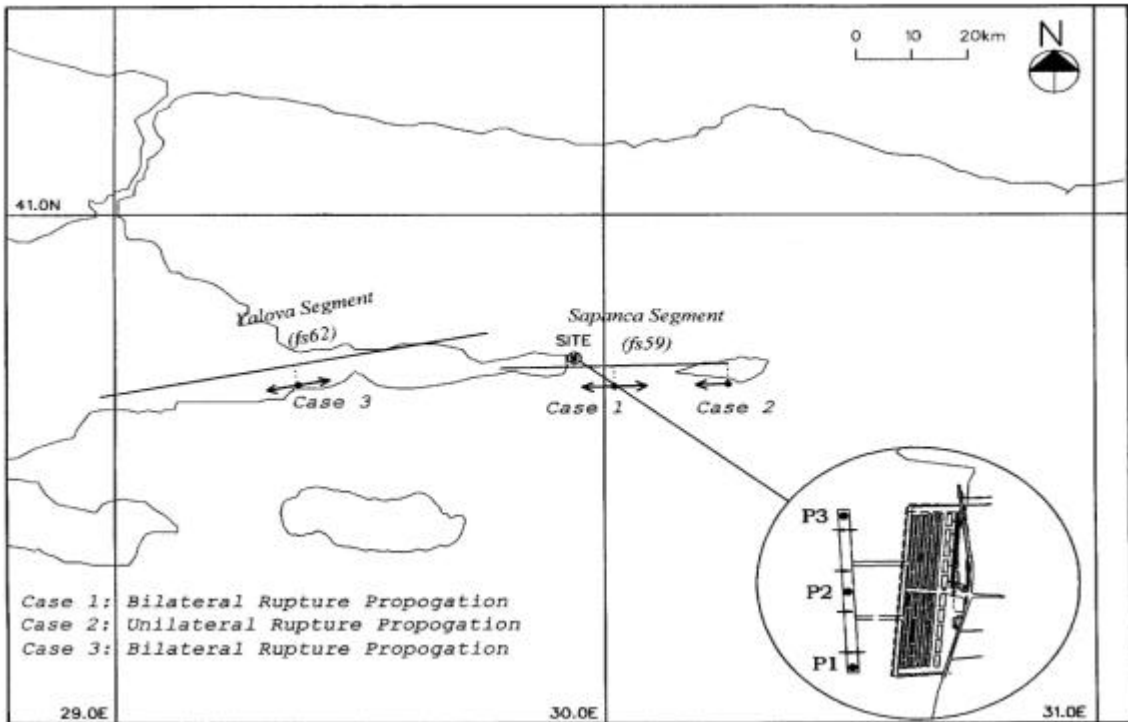


Figure 2 Modeled rupturing segments of the North Anatolian fault

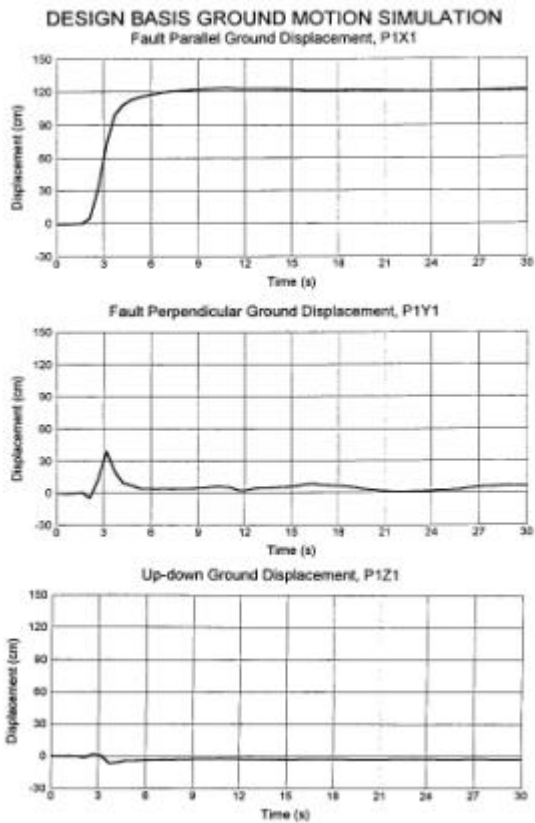


Figure 3 The fault parallel, fault perpendicular and up-down displacement components associated with the 'design basis' simulation

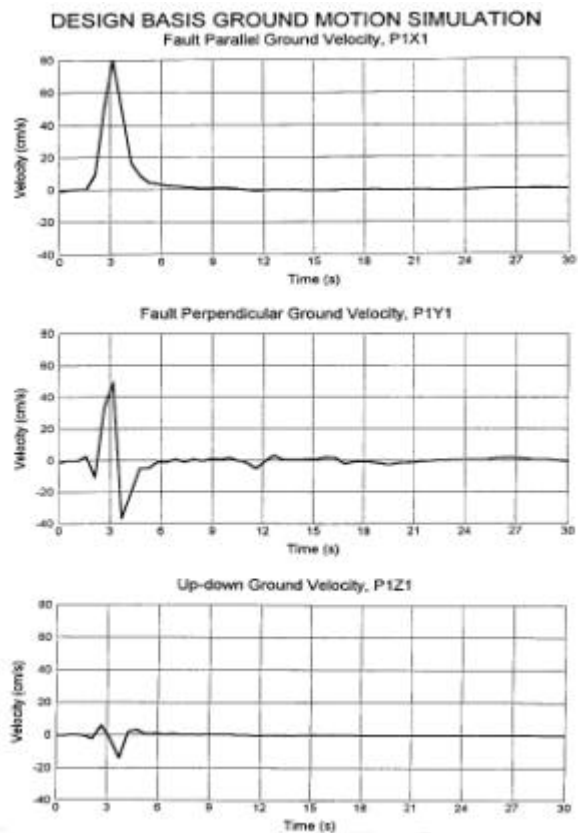


Figure 4 The fault parallel, fault perpendicular and up-down velocity components associated with the 'design basis' simulation

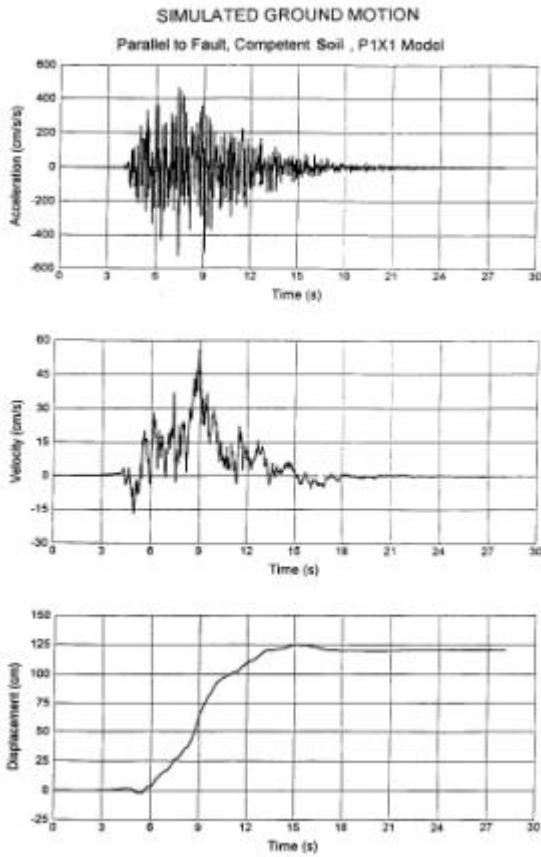


Figure 5 Simulated ground motion based on P1X1 model

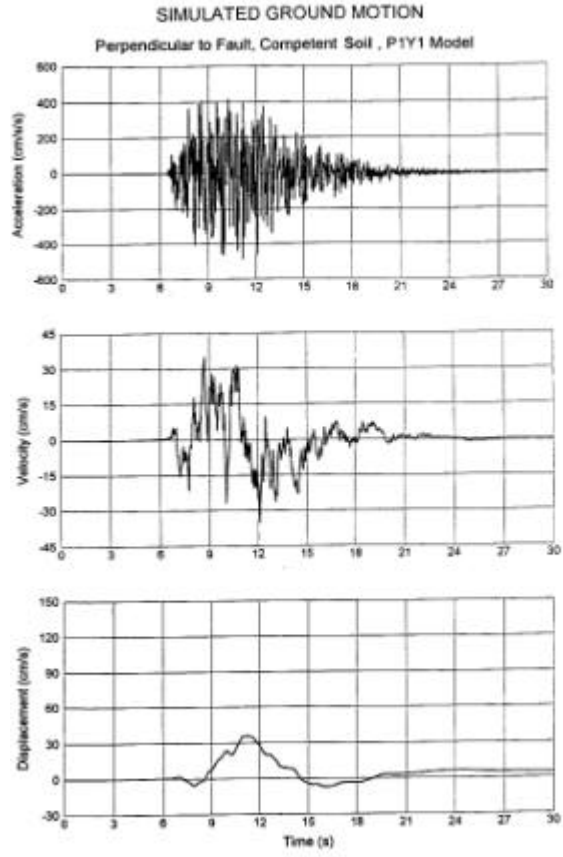


Figure 6 Simulated ground motion based on P1Y1 model

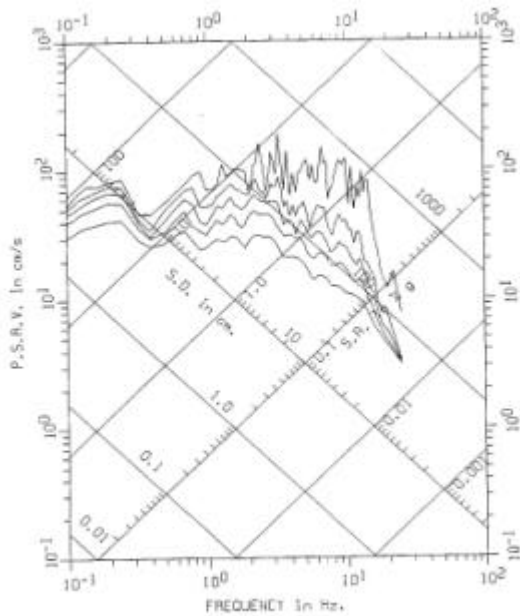


Figure 7 Response spectrum associated with the simulated ground motion based on P1X1 model (0, 2, 5, 10 & 20% damping ratio)

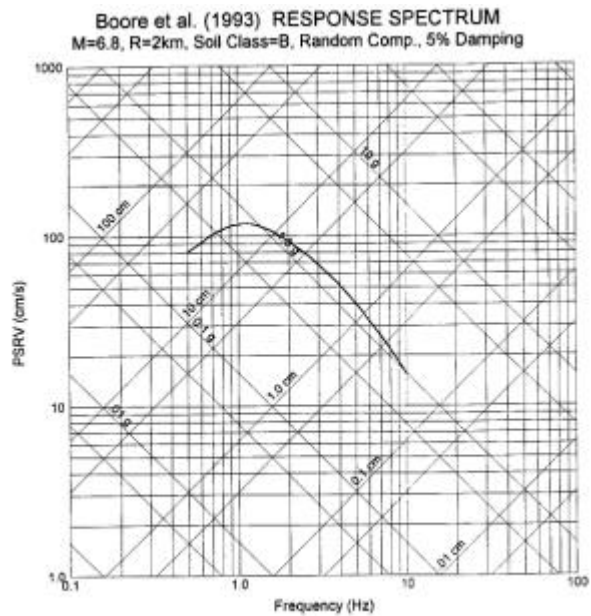


Figure 8 Empirical PSRV response spectrum associated with the design basis earthquake scenario (M=6.8, d=2 km) (Boore et al., 1993 attenuation, 5% damp)